iScience

CellPress
OPEN ACCESS

Article

Increasing the robustness and crack resistivity of high-performance carbon fiber composites for space applications

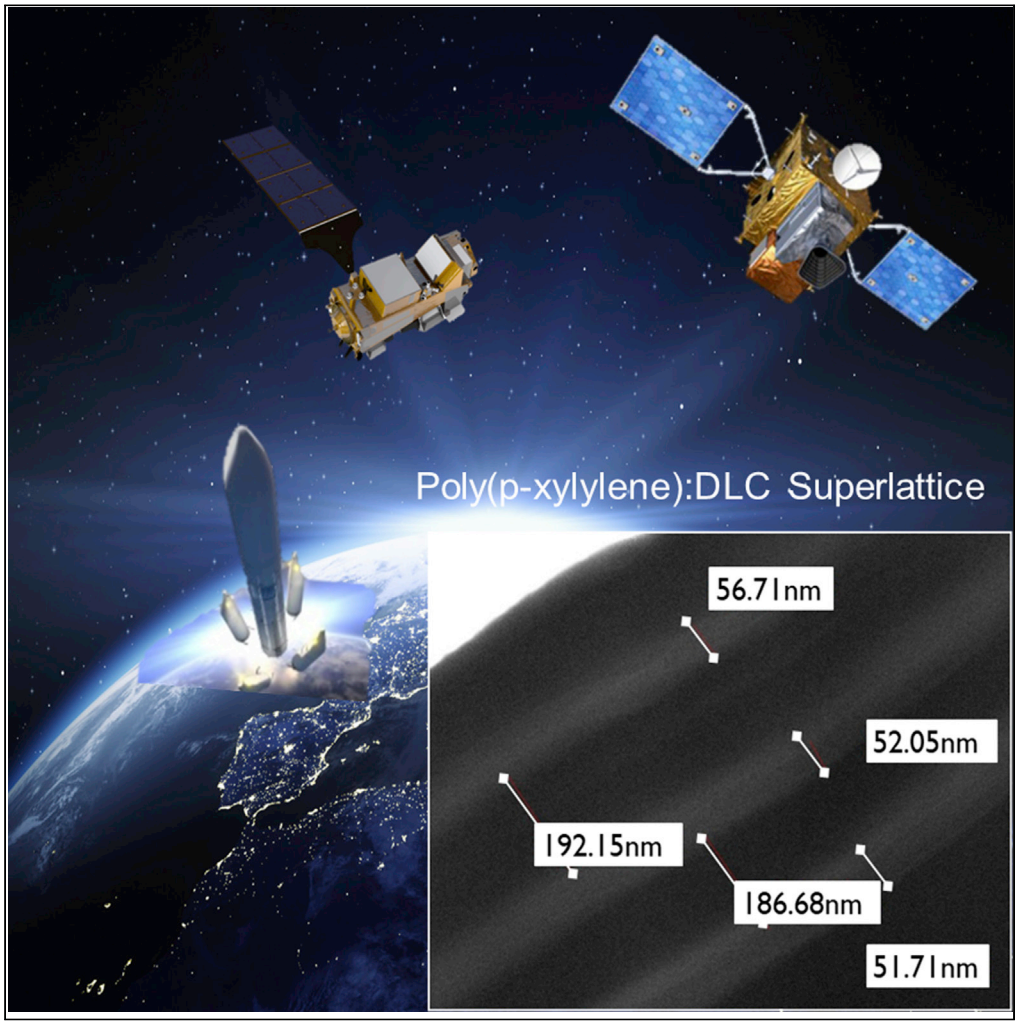

Michal Delkowski, Christopher T.G. Smith, José V. Anguita, S. Ravi P. Silva

s.silva@surrey.ac.uk

Highlights

Plasma-enhanced cross-linked poly(p-xylylene) (PECLP):DLC superlattice is deposited

PECLP exhibits ~10 times higher elastic modulus compared to classic poly(p-xylylene)

PECLP:DLC barrier provides near-zero stress conditions for use on composites

Enhanced composites exhibit mechanical integrity and improved crack resistivity

Delkowski et al., iScience *24*, 102692
June 25, 2021
https://doi.org/10.1016/j.isci.2021.102692

iScience

CellPress
OPEN ACCESS

Article

Increasing the robustness and crack resistivity of high-performance carbon fiber composites for space applications

Michal Delkowski,[1,2] Christopher T.G. Smith,[1] José V. Anguita,[1] and S. Ravi P. Silva[1,3,*]

SUMMARY

The endeavors to develop manufacturing methods that can enhance polymer and composite structures in spacecraft have led to much research and innovation over many decades. However, the thermal stability, intrinsic material stress, and anisotropic substrate properties pose significant challenges and inhibit the use of previously proposed solutions under extreme space environment. Here, we overcome these issues by developing a custom-designed, plasma-enhanced cross-linked poly(p-xylylene):diamond-like carbon superlattice material that enables enhanced mechanical coupling with the soft polymeric and composite materials, which in turn can be applied to large 3D engineering structures. The superlattice structure developed forms an integral part with the substrate and results in a space qualifiable carbon-fiber-reinforced polymer featuring 10–20 times greater resistance to cracking without affecting the stiffness of dimensionally stable structures. This innovation paves the way for the next generation of advanced ultra-stable composites for upcoming optical and radar instrument space programs and advanced engineering applications.

INTRODUCTION

Space discovery, exploratory, and monitoring programs require component and structural coatings to ensure critical mission performance under harsh environments (Ghidini, 2018). Space-bound coatings often drive and facilitate technological developments, in which applications often branch into further terrestrial implementations. These coatings must provide functionality such as mechanical and chemical protection while simultaneously maintaining their mechanical integrity under extreme test, launch, and space conditions (Holynska et al., 2018). The European Space Agency, National Aeronautics and Space Agency (NASA), and other institutions require such coatings for various electronic, optoelectronic, mechanical, and instrument applications on a range of missions including Sentinel, Earth Observation, Navigation and Science (ENS), Synthetic Aperture Radar, and deep-space missions. Applications that require such enhancement include instruments and spacecraft structures as well as mirrors, solar cells, microelectromechanical systems (MEMSs) and nanoelectromechanical systems (NEMSs), printed circuit boards (PCBs), drive mechanisms, and structural and non-structural components (Figure 1) (Fan et al., 2015; Butler, 2014; Reichhardt, 2002; Sanderson, 2008; Gondoin, 2007; Battersby et al., 2018; Gibney, 2013; Burnol et al., 2019; Raspini et al., 2018). Furthermore, initiatives have called for new designs and manufacturing approaches to integrate nanotechnologies and conceptually new materials to build advanced and adaptive spacecraft (Levchenko et al., 2018).

Hard and robust materials such as diamond-like carbon (DLC) thin films offer tunable mechanical (Young's modulus $\lesssim$500 GPa, hardness $\lesssim$100 GPa) and electrical (dielectric constant: 2.5–6.5) properties which can be used to extend the lifetime of spacecraft missions (Silva, 2003; Prelas et al., 1998; Marques et al., 2003; Silva et al., 2002; Robertson, 1986; Dasgupta et al., 1991). In addition, superlattice materials have been found useful for a broad range of engineering applications (Zhang et al., 2018; Tsu, 2010). For example, superlattices consisting of thin layers of DLC can be used to increase the mobility of charge carriers, varying the optical band gap (~1.5–5 eV) (Silva et al., 1994; McIntosh et al., 2016), for instruments and high-frequency devices (Utsunomiya et al., 2013; Bhattacharyya et al., 2006; Dong et al., 2019; Srinivasan et al., 2007; Gurnett et al., 1995). However, these materials incur high intrinsic stresses, which make them vulnerable to mechanical failure by cracking or flaking (Abadias et al., 2018; Ali et al., 2015; Khanna, 2010). Recent

[1]Advanced Technology Institute, Department of Electrical and Electronic Engineering, University of Surrey, Guildford, Surrey GU2 7XH, UK

[2]Airbus Defence and Space GmbH, Claude-Dornier-Strasse, 88090 Immenstaad, Germany

[3]Lead contact

*Correspondence: s.silva@surrey.ac.uk

https://doi.org/10.1016/j.isci.2021.102692

Figure 1. Examples of Earth Observation missions and spacecraft sub-systems requiring coatings
Space equipment and electronics such as PCB's for tin whisker growth mitigation, carbon-fiber-reinforced polymer (CFRP) dimensionally stable structures, optical mirrors, spectrometers, detectors, space mechanisms, and others.

developments have shown that poly(p-xylylene) flexible layers are able to couple and diffuse the stress between the surface of the carbon-fiber-reinforced polymer (CFRP) and the DLC barrier layers, providing integrated solutions for moisture and outgassing barriers in dimensionally stable CFRP structures (Anguita et al., 2020). For space structures that support optics in ENS missions, these must be ultra-stable and therefore virtually insensitive to environment changes that can be induced by moisture, temperature, and pressure effects on ground and over the mission lifetime. Furthermore, over the last decades, the increasing stability requirements resulted in the use of much stiffer carbon fibers going from 350 GPa to beyond 650 GPa up to 935 GPa (PITCH based, with up to 99.9% of carbon content) for ultra-high modulus (UHM) carbon fibers and the use of vacuum infusion processes that ensures minimum 60% of fiber volume content in the composite matrix. These UHM fibers offer high thermal conductivity (up to 800 W/mK) and high electrical resistivity (~1–1.5 μΩm) but are very brittle and difficult to handle. As a result, it is difficult to embed hard protective coatings on these fibers due to the buildup of stress along the fiber direction, giving the rise to cracks that propagate perpendicular to the fibers. These crack propagations are enhanced by differences in coefficient of thermal expansion (CTE) between the composite matrix and hard layer materials. The poly(p-xylylene), with the CTE of ~35–69 ppm and elastic modulus of ~0.5–2.7 GPa, is flexible (40% elongation at break) and intermediates properties between the hard layers and composite substrates. However, commercially deposited poly(p-xylylene) derivates are not sufficiently mechanically stable, chemically inert, or hard enough to permit matching of the coatings into the various shape substrates. To improve this mechanical coupling, adhesion promoters are necessary (Mitchel et al., 2006; Wypych, 2018), which in turn facilitates contaminants being trapped inside the coating with no possibility of removal in situ or after the process. Using elevated temperatures has been shown to strengthen their structure; however, this restricts some material applications and can only be achieved by breaking the vacuum, specifically for flat samples (Hong et al., 2015).

In this article, we present a plasma-enhanced cross-linked poly(p-xylylene) (PECLP):DLC superlattice barrier composite that is harder, more mechanically and environmentally stable than space-qualified CFRP composites. The PECLP layers exhibit ~10 times higher elastic modulus compared to the classically deposited poly(p-xylylene) as a result of the near zero-stress conditions. The deposition method does not require adhesion promoters and enables in situ contamination cleaning, necessary for ultra-sensitive scientific instruments. The room temperature deposition process also enables suitable matching between harder layers such as DLC layers and a CFRP substrate which in turn permits new space qualifiable composite structures. The ultra-thin multilayer structure (<1.5 μm) is more robust, wear resistant, and capable to withstand the static and dynamic loads that a space instrument structures may encounter during tests, launch, and spaceflight (DeLombardet and McPherson, 1997; Tryggvason et al., 2001). The resulting PECLP:DLC superlattice-matched structural composites can withstand higher constant and vibration loads than the space-qualified CFRP substrate itself. The ultra-thin nature of mechanically integrated multilayer barrier structure has no negative effect on the overall strength and structure stiffness. This constitutes a significant improvement over previous proposed composite

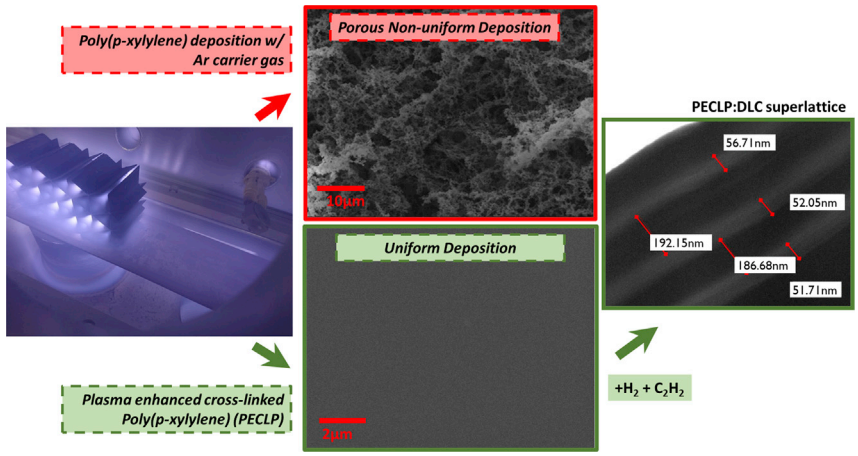

Figure 2. Poly(p-xylylene) single and multilayer coating deposition process

Images demonstrating the plasma deposition of single or multilayer structures consisting of PECLP and DLC layers in one step and without vacuum interruption on a complex 3-D component (CFRP honeycomb). The image highlighted in red shows an example of classical poly(p-xylylene) using an argon carrier gas to increase deposition range, which leads to an porous non uniform distribution. The contrasting images highlighted in green show the uniform high-quality film of PECLP and subsequent PECLP:DLC superlattice film cross section.

and polymer coatings for space, such as metals or ceramics, whereby hard deposited layers easily crack or spall due to inability to conform with the substrate stresses (Banks et al., 1985; Banks et al., 1984; Dever et al., 2002; Dever and de Groh, 2002). The deposition system allows for the deposition of PECLP:DLC superlattice layers over 3D structures and can also be deposited without requiring line of sight from the source materials, resulting in a clean multilayer-coated advanced CFRP material.

RESULTS

Deposition and morphological analysis

Poly(p-xylylene) films are often realized by electrochemical polymerization or a vapor deposition process (VDP) using the Gorham method (Ishaque et al., 2002; Jeong et al., 2002), which splits a dimer molecule into two monomers at high temperature (~650°C +) prior to room temperature deposition. Vaporized dimers undergo pyrolysis in a pyrolysis furnace at this elevated temperature to form reactive radicals. However, it is difficult to obtain a uniform coating on large, complex shape components in a single process run. Also, monomers can deposit on the vacuum chamber walls, causing contamination and coating speed reduction between cycles. Strategies that involve the introduction of carrier gases that may be used to improve uniformity can influence collision mechanics and ultimately film morphology. This was verified in this work, where Figure 2 depicts a premature nucleation in the gas phase, instead of polymerization on the substrate, which results in a porous non-uniform deposition. This is likely caused by increased pressure in the chamber due to the presence of the carrier gas, increasing the likelihood of monomer collisions in the gas phase. Furthermore, traditionally deposited poly(p-xylylene) polymers are not sufficiently tough and mechanically stable to conform on various substrates and hard films such as DLCs for advanced applications. This causes poor adhesion and results from weak thermal properties and water sensitivity which is further enhanced by exposure to harsh environments. These issues have been repeatedly reported in the past (Ortigoza-Diaz et al., 2018; Nichols et al., 1998).

To overcome them, a virtual live electrode plasma enhanced chemical vapour deposition (PECVD) process is used here, where monomers pass through low-pressure plasma at room temperature, forming excited radicals by chemical activation and polymerize on the substrates. The substrate is coupled to the electrical radiofrequency power supply (driven by 13.56 MHz) to the plasma creating a virtual electrode on which polymerization occurs. This PECLP process does not require adhesion promoters due to plasma activation resulting in improved substrate adhesion. Figure 2 shows the typical uniform morphology of PECLP across a substrate after deposition. This is likely because the plasma deposition reduces collisions between activated monomers and molecular contaminants within the chamber which cause premature nucleation and poor film quality. Plasma activation of the monomers also results in enhanced cross-linking of the poly(p-

xylylene) where C-H bonds can cleave and subsequently bind with activated monomers, thereby increasing the cohesion of the bonds. Consequently, free H-side groups or monomers react with each other resulting in a denser three-dimensional network, so the resulting polymers are chemically linked to each other. Fourier transform infrared (FTIR) analysis (Figure S1) shows that the weak plasma does not damage the polymer molecular structure, where all infrared absorption peaks from the analytical-grade poly(p-xylylene) from CH-stretch band are visible, including aromatic and aliphatic compounds with pronounced stronger bands at ~1690–1700 cm^{-1}(C=C stretch) and between 3200 and 2800 cm^{-1}(C-H stretch). Because of the stable low pressure plasma process and no molecular collisions present, the polymer can achieve more similar content of each monomer moiety resulting in better thermal stability which is further analyzed and compared to the classical VDP of poly(p-xylylene). Here, the activation step has been realized in situ by plasma, whereas previous studies showed (Moss and Greiner, 2020) that additional groups such as esters or UV post-treatment can be introduced in order to enable this enhanced linkage and thus stability.

With further analysis, the collected volatile condensable material (CVCM) values, determined from microvolatile condensable material measurements, show 0.000% CVCM measured for PECLP-coated samples compared to 0.03% from the classically deposited poly(p-xylylene) films suggesting a densification in PECLP as postulated. The values for classically deposited poly(p-xylylene) films are consistent with previously reported results by NASA (NASA, 2017) and suggest a change in the polymer network under exposure to these test conditions. These negligible CVCM results also demonstrate that PECLP has improved barrier effectiveness under vacuum and varied temperature conditions. Typically, VDP poly(p-xylylene) can survive continuous service temperature of 333K and short-term temperature of 353K, whereas PECLP has been shown to be stable across a wide temperature range along with continuous temperature of 398K validated during thermal vacuum cycling and gravimetric measurements. Furthermore, experiments have shown that hard coatings deposited on PECLP, whereby PECLP acts as an intermediate buffer layer, passed adhesion tape tests, even after multiple thermal stress cycles from 77K to 523K which simulates greater temperature fluctuations than specified from spaceflight validation.

By combining with a traditional PECVD DLC deposition process, the PECLP layer can be tuned to intermediate the mechanical expansion properties between the substrate and hard layer materials such as DLCs, which alone exhibit poor mechanical matching to the substrate. This compatible multilayer PECVD process allows the formation of enhanced and conformal coatings over large, 3D components in a one coating run after manufacture and assembly of the final product before satellite launch. This ability is demonstrated in Figure 2, where a 3D honeycomb CFRP core assembly, part of the optical bench sandwich, is shown which is coated in one single multi-step deposition stage. The coating structure consists of PECLP and DLC multilayers that are mechanically coupled. A cross section of this PECLP:DLC superlattice is depicted in Figure 2. This demonstrates that the PECLP:DLC superlattice is able to completely surround the entire surface of complex 3D composite components, thereby forming the nanocoating on its surface. This one single coating run is realized without interrupting the plasma which allows for continuity of the growth process, no layer oxidation, and no molecular chain scission for complete conformal and mechanical integrity of the single PECLP and combined PECLP:DLC superlattice-coated structures.

Film mechanical properties and nano-indentation analysis

Ex situ nano-indentation analysis determines the hardness, elastic modulus, and the plastic index (ratio of plastic deformation over the overall deformation including elastic recovery) of a single deposited PECLP layer and investigates the contact pressure (the stress resulting from the load applied within the projected area of the tip in contact with the materials) as a function of depth through a multilayer PECLP:DLC coating structure. A minimum of three PECLP-coated specimens were indented to a maximum depth of around 10% of their thickness (≈ 50 nm) to avoid substrate effects. Figure 3A shows that the PECLP samples exhibit a tenfold greater elastic modulus (~12 GPa, red bars) and approximately twofold greater hardness (~1 GPa, blue bars) compared to the classical VDP poly(p-xylylene) films (~1.2 GPa and 0.4 GPa, respectively).The values for the classically VDP poly(p-xylylene) films were commonly and consistently reported (Mulpuri et al., 2012; Li et al., 1992; Zhang et al., 1995). This demonstrates the effectiveness of a virtual electrode PECVD process to manufacture the PECLP structures presented and the enhancements of PECLP over traditional poly(p-xylylene).

Figure 3B further demonstrates the PECLP ability to compensate for high compressive residual stresses of the DLC coatings which solely attained values greater than ~80 GPa. This depicts measured contact

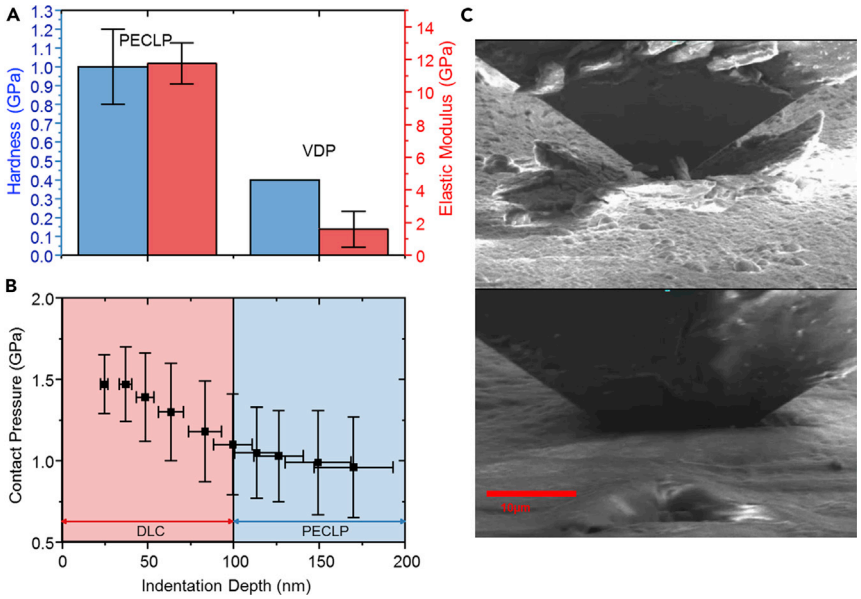

Figure 3. Ex situ and in situ nanoindentation test results on a single PECLP and multilayer PECLP:DLC superlattice coating structure

(A) Summary of mechanical properties (elastic modulus and hardness) for the single plasma-enhanced cross-linked poly(p-xylylene) (PECLP) layers compared to the classically vapor-deposited poly(p-xylylene). Error bars represent standard deviations from minimum three samples and 75 measurement points. Deposited PECLP layers show greater elastic modulus and hardness demonstrating enhanced performance over traditional poly(p-xylylene).

(B) Measured contact pressure (stress relaxation) as a function of depth for the multilayer PECLP:DLC coating structure. The PECLP shows the ability to relax the high DLC stresses providing a near-zero stress condition which results in enhanced mechanical integrity. Error bars represent standard measurement errors.

(C) Scanning electron microscopy (SEM) images during the testing showing failure and fracture modes with cracks starting to occur at 160 mN of force for CFPR with 4 PECLP:DLC layers (top image) and at ~10–20 mN of force for uncoated CFPR.

pressure and measured elastic modulus of the multilayer PECLP:DLC coatings as a function of the indentation depth. The first loading cycle values were extracted from the first 25% of the top DLC layer, yielding a contact pressure and apparent elastic modulus of about 1.5 and 17.2 GPa, respectively. With the load increase (higher indentation depth), both the contact pressure and apparent elastic modulus decrease as the stress field is effectively coupled by the PECLP layers. This shows that the PECLP is able to level the contact pressure to a value of about 1 GPa, minimizing both the structural and thermal stresses of the hard DLC layer, which now can be deposited with the near-zero stress conditions. This allows harder layers such as DLC to be deposited on soft substrates, including polymers and composites used in the space industry, compensating their surface anisotropy properties, which overcome the issues previously stated.

This is further evidenced through dilatometry measurements for operational environment between −40°C and 80°C (on 8 DLC:PECLP multilayer coated UD0° and UD90° CFRPs). This allows us to study the length change phenomena of materials under given conditions. As a result, the deflections have been monitored in both directions and the PECLP:DLC multilayer stresses (σ_f) determined by fitting to the Stoney's equation:

$$\sigma_f = \frac{E_s * {h_s}^2}{6 * (1 - V_s)} * \frac{{h_f}^2}{h_s} * \left(\frac{1}{R} - \frac{1}{R_0}\right)$$

where E_s, h_s, and V_s are the Young's modulus, thickness, and the Poisson's ratio of the substrate, respectively, whereas h_f is the PECLP:DLC multilayer coating thickness, and R and R_0 are the radii of curvature before (R) and after (R_0) temperature stress application.

This shows measured stresses of −112.06 and −153.70 MPa for UD0° and UD90°, 8 multilayer PECLP:DLC coated composites, respectively. In comparison, coated composites with single DLC layer immediately delaminated as a result of high compressive stress. This demonstrates the capability of PECLP for leveling the

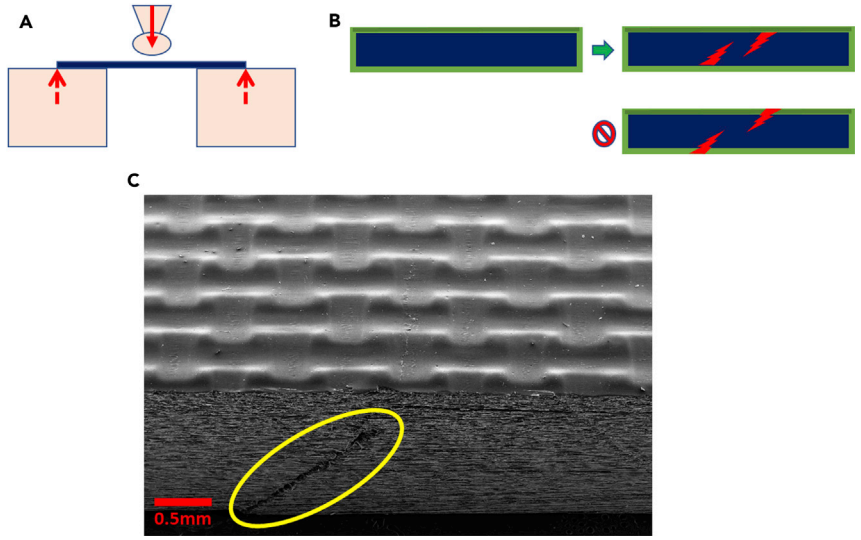

Figure 4. Static three-point bending tests on PECLP:DLC superlattice-coated ultra-high-modulus space CFRPs

(A) Schematic showing a typical three-point bending test arrangement (in compliance with DIN ISO 14125).

(B) Images illustrating coated composite (coating as a thin green layer) and possible tensile or compression failure modes (for UD90° or UD0° lay-up, respectively) that may occur due to the loading. This is failure inside the bulk CFRP material or in the coating.

(C) SEM image of the PECLP:DLC superlattice-coated CFRP after loading up to approx. 260[N] (~80% of the maximum CFRP strength) showing crack initiation (highlight) inside the bulk CFRP and no cracks appearing on the PECLP:DLC 4-coating layers.

stresses and shows that, with the increase of layer numbers, the stresses are mechanically coupled, with further equilibration across the entire coating, and thereby the stresses are decreased, consistent with the ex situ nanoindentation measurements demonstrated in the work.

In situ nanoindentation of single PECLP and multilayer PECLP:DLC (2, 4, and 8 barrier layers) coating structures deposited on CFRP and silicon materials was used to investigate the failure mode and coating deformation behavior during loading. The uncoated CFRP substrates were also tested to compare coating dislocation, robustness, and handling capability from a space structural perspective. Loading displacement curves showed that with the increase of PECLP layers in the multilayer, the mechanical properties (hardness and elastic modulus) also improve, and thus, stresses are decreased which is consistent with previous ex situ nanoindentation test results. Uncoated and single DLC-coated CFRPs exhibit low resistance, either cracking or delaminating after ~10 and 20 mN of forces, respectively. In comparison two, four, and eight multilayers (PECLP:DLC) coated on CFRPs showed crack initiation at approximately 80, 160, and 200 mN of forces, respectively (Figures 3C and S2). These values are 10–20 times higher and demonstrate the PECLP coating effectiveness to form enhanced and robust multilayer composite structures, which are mechanically more stable and resistant than the current state-of-the-art qualified space structural CFRPs.

Static, vibration, and wear resistivity tests for spaceflight

Mechanical static and vibration tests show PECLP-based coating capability to withstand static and dynamic loads that the space structures encounter during tests, launch, and in-orbit conditions. Three-point bending tests (Figure 4) examined the flexural properties and material strength of PECLP-based coatings. Four and eight PECLP:DLC barrier layers deposited on CFRP were first tested with up to ~80% of the maximum bulk material strength (~260 N). Scanning electron microscopy shows the rupture initiated inside the bulk CFRP plies, while PECLP:DLC coatings remained intact. This confirms very robust coating structure and mechanical integrity of the multilayer coatings—CFRP system. Furthermore, this also shows that the weak point is now the bulk composite material as a result of exceeding its maximum strength, rather than the multilayer coatings. Flexural strength testing of unidirectional (UD0° and UD 90°) CFRP samples showed no differences between coated (with 4 and 8 layers) and uncoated substrates (528.8–543 MPa and 32–33.6 MPa for UD0° and UD90°, respectively) as expected. This is because the coating is insignificantly thin compared to the bulk of the sample and therefore does not affect the flexural strength. Instead,

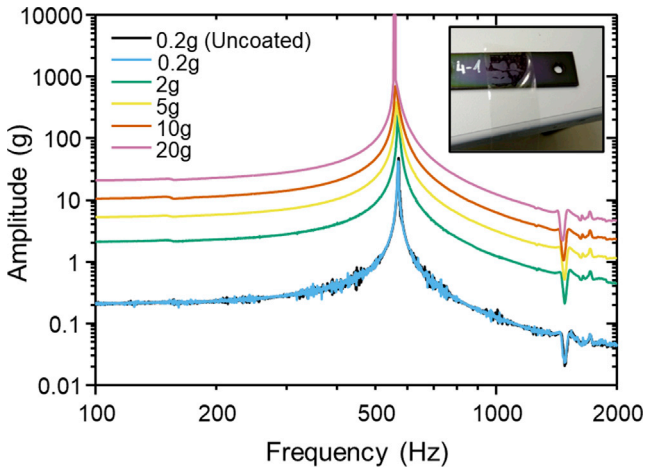

Figure 5. Vibration test results for spaceflight and verification of coating robustness

Resonant frequencies for given amplitudes on uncoated and PECLP:DLC superlattice-coated CFRP substrates demonstrating no influence on the stiffness of highly dimensionally stable CFRPs due to ultra-thin coating nature. Tests confirm the coating durability and characteristics demonstrating no frequency shift after applying high-level amplitude of 20g and further returning to 0.2g (sweep rate between 2oct/min). Inset shows the adhesion tape test after vibration and thermal cycling tests (−50°C, 80°C) which demonstrates no coating loss and further robustness of the PECLP:DLC layers.

such properties are predominated by the fiber orientation in the resin system matrix that feature high stiffness and strength in the fiber direction, while low stiffness and strength perpendicular to them. The rupture tests show no multi-cracking, flaking, or delamination of the PECLP:DLC coatings which remained intact along the surface. This demonstrates their applicability for close to contamination-sensitive equipment accommodation from an industrial perspective (Brown et al., 2019).

Cantilever vibration beam tests were conducted to determine a dynamic modulus of structural components and subsequently used to evaluate coating robustness. The dynamic modulus (E_d) was calculated fitting to the equation:

$$E_d = \left(\frac{L}{\lambda}\right)^4 * \frac{4\pi^2 * F_r^{\,2} * \rho A}{I}$$

where L is the length of the beam, ρ is the density of the material, A is the cross-sectional area, and F_r is the resonant frequency. The loss modulus from the entire system was calculated based on the frequency difference ($f_2 - f_1$) for the given amplitudes. These included correction factors for the rotary inertia and shear deformation effects added to the Bernoulli-Euler theory according to the Timoshenko model (Timoshenko and Gere, 1989). The measured average total modulus for uncoated and PECLP:DLC superlattice-coated UHM CFRP (UD0° and UD90°) structural components is summarized in Table S1. These results (~321 GPa and ~5 GPa for UD0° and UD90° samples, respectively) are in close agreement with the static tests and show that with adequate coating design and by coupling coatings to the substrates the stiffness of dimensionally stable space structure composites is not influenced, as the ultrathin coating nature cannot shift frequency significantly.

The samples were further examined to the accelerated test sequence ranging from 0.2g to 20g (Earth's gravity acceleration). Figure 5 shows that the highest peak recorded in the first mode exceeded 10^4 g with additional mass on the free end of the beam, which even overloaded the maximum readable values by accelerometers. This demonstrates PECLP:DLC coating robustness from a structural perspective and shows its ability to survive even higher quasi-static, sine and random vibration loads than the support and space instrument structures typically experience in test, launch, and in-orbit conditions. No cracks or delamination was detected, and by further returning from 20g to 0.2g, the frequency characteristics confirmed unchangeable coated CFRP behavior, with no frequency shift.

Mass measurements and adhesion tape tests (as depicted in the inset of Figure 5) after static, dynamic, and thermal cycling stress tests (range: −50°C, 80°C) confirmed coating robustness and integrity. Additional

cubic masses and cables which represented space harness rubbing against coated structures showed no appreciable wear volume loss of the enhanced PECLP:DLC coatings. These space harnesses are used to convey the electrical power or signal in the satellite systems, with typically more than 50,000 connections located for large spacecraft that have to be accommodated around the structures and sub-systems. This shows the multilayer coating effectiveness from a mechanical perspective and its ability robustness to being intact during all satellite assembly, integration, tests, and finally launch and in-orbit simulated conditions. This paves the way for the next generation of advanced composite structures which are superior in strength and stiffness and offer barrier protection functionalities by the multilayer barrier coatings.

DISCUSSION

A technology is presented in this study that enables enhanced cross-linked poly(p-xylylene) manufacturing that enables coupling of hard layer materials to the soft and anisotropy substrates in a single deposition step, forming mechanically robust superlattice composite structures. This is made possible by RF-coupled, low-pressure, and low-temperature plasma processes to the substrate materials that behave as one virtual electrode. The formed PECLP:DLC superlattice structures feature higher elastic modulus, improved temperature, and shear resistance resulting in evasion of dislocations compared to the classically deposited poly(p-xylylene) and space-qualified CFRP materials. The plasma-assisted process prevents contaminant formation that can be prematurely bound in the monomers or be trapped in the films. This study demonstrates the ability for nano-barrier use in contamination-sensitive areas such as optical instruments, mirrors, electronics, and similar components applicable and utilized for space exploration. The PECLP layers enable stress relaxation (coupling) in the hard layer materials which can be mechanically matched to the conventional space-qualified CFRP, resulting in a new generation of advanced composites with superior stiffness, strength, and wear-resistant properties. This allows coating application for both structural and non-structural components. Barrier performance and further coating protection and functionalities can be imparted to the bulk substrate materials. The PECLP:DLC barrier structures achieve this with the very low thickness, not disturbing mechanical properties of the space-qualified CFRPs. Space-borne developments like this often drive and facilitate technological improvements, branching to other terrestrial applications such as automotive, electronics, wind energy, and aeronautic industries, generally raising material properties to the next level, thereby paving the way for novel applications.

Limitations of study

While the use of PECLP and PECLP:DLC superlattices may be applied to other materials providing useful effects, this study is limited to polymer and composite materials.

STAR★METHODS

Detailed methods are provided in the online version of this paper and include the following:

- KEY RESOURCES TABLE
- RESOURCE AVAILABILITY
  - Lead contact
  - Materials availability
  - Data and code availability
- METHOD DETAILS
  - Deposition
  - Thermal-vacuum outgassing tests for screening of space materials
  - Thermal-vacuum cycling tests
  - Adhesion verification w/wo thermal-shock test
  - Nano-identation characterization
  - Thickness inspection measurements
  - Dilatometry measurements
  - Three-point bending tests
  - Vibration tests

SUPPLEMENTAL INFORMATION

Supplemental information can be found online at https://doi.org/10.1016/j.isci.2021.102692.

ACKNOWLEDGMENTS

The authors would like to thank Dr. David Cox and Dr. Vlad Stolojan for the production of sample cross sections and electron microscopy, respectively. The authors would like to thank Airbus for financial contributions to the project.

AUTHOR CONTRIBUTIONS

The program was designed by authors and all of them contributed to various research and testing phases of the project. The paper was written by all authors that contributed and commented on it.

DECLARATION OF INTERESTS

The authors declare no competing interests.

Received: February 11, 2021
Revised: May 17, 2021
Accepted: June 3, 2021
Published: June 25, 2021

REFERENCES

Abadias, G., Chason, E., Keckes, J., Sebastiani, M., Thompson, G.B., Barthel, E., Doll, G.L., Murray, G.E., Stoessel, C.H., and Martinu, L. (2018). Stress in thin films and coatings: current status, challenges, and prospects. J. Vac. Sci. Technol. A *36*, 020801. https://doi.org/10.1116/1.5011790.

Ali, R., Sebastiani, M., and Bemporad, E. (2015). Influence of Ti–TiN multilayer PVD-coatings design on residual stresses and adhesion. Mater. Des. *75*, 47–56. https://doi.org/10.1016/j.matdes.2015.03.007.

Anguita, J.V., Smith, C.T.G., Stute, T., Funke, M., Delkowski, M., and Silva, S.R.P. (2020). Dimensionally and environmentally ultra-stable polymer composites reinforced with carbon fibres. Nat. Mater. *19*, 31–322. https://doi.org/10.1038/s41563-019-0565-3.

Banks, B.A., Mirtich, M.J., Rutledge, S.K., and Swec, D. (1984). Sputtered coatings for protection of spacecraft polymers. In 11th International Conference on Metallurgical Coatings (AVS) (NASA TM-83706).

Banks, B.A., Mirtich, M.J., Rutledge, S.K., Swec, D.M., and Nahra, H.K. (1985). Ion beam sputter-deposited coatings for protection of spacecraft polymers in low earth orbit. In 23rd Aerospace Sciences Meeting (AIAA) Ren, Nevada (NASA TM-87051). https://doi.org/10.2514/6.1985-420.

Battersby, C., Armus, L., Bergin, E., Kataria, T., Meixgner, M., Pope, A., Stevenson, K.B., Cooray, A., Leisawitz, D., Scott, D., et al. (2018). The origins space telescope. Nat. Astron. *2*, 596–599. https://doi.org/10.1038/s41550-018-0540-y.

Bhattacharyya, S., Henley, S.J., Mendoza, E., Gomez-Rojas, L., Allam, J., and Silva, S.R.P. (2006). Resonant tunnelling and fast switching in amorphous-carbon quantum-well structures. Nat. Mater. *5*, 19–22. https://doi.org/10.1038/nmat1551.

Brown, A., Bernot, D., Ogloza, A., Olson, K., Thomas, J., and Talghader, J. (2019). Physical origin of early failure for contaminated optics. Sci. Rep. *9*, 635. https://doi.org/10.1038/s41598-018-37337-5.

Burnol, A., Aochi, H., Raucoules, D., Veloso, F.M.L., Koudogbo, F.N., Fumagalli, A., Chiquet, P., and Maisons, C. (2019). Wavelet-based analysis of ground deformation coupling satellite acquisitions (Sentinel-1, SMOS) and data from shallow and deep wells in southwestern France. Sci. Rep. *9*, 8812. https://doi.org/10.1038/s41598-019-45302-z.

Butler, D. (2014). Earth observation enters next phase. Nat. News *508*, 160. https://doi.org/10.1038/508160a.

Dasgupta, D., Demichelis, F., and Tagliaferro, A. (1991). Electrical conductivity of amorphous carbon and amorphous hydrogenated carbon. Philos. Mag. B *63*. https://doi.org/10.1080/13642819108205558.

DeLombardet, R., and McPherson, R. (1997). Microgravity Environment Description Handbook, NASA Technical Memorandum (NASA Technical Reports Server).

Dever, J., and de Groh, K. (2002). Vacuum Ultraviolet Radiation and Atomic Oxygen, Durability Evaluation of HST Bi-stem Thermal Shield Materials (NATA/TM-2002-211364).

J. Dever, C. Semmel, D. Edwards, R. Messer, W. Peters, A. Carter, D. Puckett. (2002). Radiation Durability of Candidate Polymer Film for the Next Generation Space Telescope Sunshield, AIAAA 2002-1564. https://doi.org/10.2514/6.2002-1564

Dong, W., Duan, W., Liu, W., and Zhang, Y. (2019). Microgravity disturbance analysis on Chinese space laboratory. npj Microgravity *5*, 18. https://doi.org/10.1038/s41526-019-0078-z.

Fan, X., Xue, Q., and Wang, L. (2015). Carbon-based solid-liquid lubricating coatings for space applications. – a review. Friction *3*, 191–207. https://doi.org/10.1007/s40544-015-0079-1.

Ghidini, T. (2018). Materials for space exploration and settlement. Nat. Mater. *17*, 846–850. https://doi.org/10.1038/s41563-018-0184-4.

Gibney, E. (2013). X-rays top space agenda. Nat. News *503*, 7474. https://doi.org/10.1038/503013a.

Gondoin, P. (2007). Astronomical opportunities. Nat. Photon. *1*, 605–607. https://doi.org/10.1038/nphoton.2007.207.

Gurnett, D.A., Persoon, A.M., Randall, R.F., Odem, D.L., Remington, S.L., Averkamp, T.F., Debower, M.M., Hospodarsky, G.B., Huff, R.L., L Kirchner, D., et al. (1995). The polar plasma wave instrument. Space Sci. Rev. *71*, 597–622. https://doi.org/10.1007/BF00751343.

Holynska, M., Tighe, A., and Semprimoschnig, C. (2018). Coatings and thin film for spacecraft thermo-optical and related functional applications. Adv. Mater. Inter. *5*, 1701644. https://doi.org/10.1002/admi.201701644.

Hong, S., Hu, X., Xu, K., Tang, C., Zhou, Y., Shuai, M., Mei, J., Zhu, Y., and Lau, W. (2015). Enhanced water vapor barrier property of poly (chloro-p-xylylene) film by formation of dense surface cross-linking layer via hyperthermal hydrogen treatment. RSC Adv. *69*. https://doi.org/10.1039/C5RA07557B.

Ishaque, M., Agarwal, S., and Greiner, A. (2002). Synthesis and properties of novel poly (p-xylylene)s with aliphatic substituents. e-Polymers *31*, 1–10. https://doi.org/10.1515/epoly.2002.2.1.442.

Jeong, Y.S., Raiter, B., Moliton, A., and Guyard, L. (2002). UV–visible and infrared characterization of poly(p-xylylene) films for waveguide applications and OLED encapsulation. Synth. Met. *127*, 189–193. https://doi.org/10.1016/S0379-6779(01)00621-X.

Khanna, V. (2010). Adhesion–delamination phenomena at the surfaces and interfaces in microelectronics and MEMS structures and packaged devices. J. Phys. D *44*, 034004. https://doi.org/10.1088/0022-3727/44/3/034004.

Levchenko, I., Xu, S., Teel, G., Mariotti, D., Walker, M.L.R., and Keidear, M. (2018). Recent progress and perspectives of space electric propulsion

systems based on smart nanomaterials. Nat. Comms. *2018*, 879. https://doi.org/10.1038/s41467-017-02269-7.

Li, H., Moshonov, A., Muzzy, J.D., and Olsen, R.A. (1992). Structures and properties of poly (p-xylylene) composites made by electrochemical and vapor deposition polymerization. Polym. Composites *13*, 402–407. https://doi.org/10.1002/pc.750130510.

Marques, F.C., Lacerda, R.G., Champi, A., Stolojan, V., and Silva, S.R.P. (2003). Thermal expansion coefficient of hydrogenated amorphous carbon. Appl. Phys.Lett. *83*, 3099. https://doi.org/10.1063/1.1619557.

McIntosh, R., Henley, S.J., Silva, S.R.P., and Bhattacharyya, S. (2016). Coherent quantum transport features in carbon superlattice structures. Sci. Rep. *6*, 35526. https://doi.org/10.1038/srep35526.

Mitchel, C.J., Yang, G., and Senkevich, J.J. (2006). Adhesion aspects of poly(p-xylylene) to SiO2 surfaces using γ -methacryloxypropyltrimethoxysilane as an adhesion promoter. J. Adhes. Sci. Technol. *20*, 1637–1647. https://doi.org/10.1163/156856106778884217.

Moss, T., and Greiner, A. (2020). Functionalization of poly(para-xylylene)s-opportunities and challenges as coating material. Adv. Mater. Inter. *7*, 1901858. https://doi.org/10.1002/admi.201901858.

Mulpuri, S.V., Shin, B., Bognitzki, M., and Greiner, A. (2012). Thermally cross-likable poly(p-xylylene) s for advanced low-dielectric applications, *macromolecular Chemistry and physics*. Bd *213*, 705–712. https://doi.org/10.1002/macp.201100558.

NASA (2017) Outgassing Data for Selecting Spacecraft Materials Online, https://outgassing.nasa.gov/.

Nichols, M.F., Hahn, A.W., and Sharma, A.K. (1998). The effect of high energy 'electrodelesś plasma polymerized methane polymers on the adhesion characteristic of poly-p-xylylene films. J. Adhes. Sci. Technol. *2*, 59–66. https://doi.org/10.1163/156856188X00066.

Ortigoza-Diaz, J., Scholten, K., Larson, C., Cobo, A., Hudson, T., Yoo, J., Baldwin, A., Weltman Hirschberg, A., and Meng, E. (2018). Techniques and considerations in the microfabrication of parylene C microelectromechanical systems. Micromachines (Basel). https://doi.org/10.3390/mi9090422.

Prelas, M.A., Popovici, G., and Bigelow, L.K. (1998). Handbook of Industrial Diamonds and Diamond Films (CRC Press). https://doi.org/10.1201/9780203752807.

Raspini, F., Bianchini, S., Ciampalini, A., Del Soldato, M., Solari, L., Novali, F., Del Conte, S., Rucci, A., Ferretti, A., and Casagli, N. (2018). Continuous, semi-automatic monitoring of ground deformation using Sentinel-1 satellites. Sci. Rep. *8*, 7253. https://doi.org/10.1038/s41598-018-25369-w.

Reichhardt, T. (2002). NASA roadmap charts route to a quarter-century of exploration. Nature *420*, 593–594. https://doi.org/10.1038/420593a.

Robertson, J. (1986). Amorphous carbon. Adv. Phys. *35*. https://doi.org/10.1080/00018738600101911.

Sanderson, K. (2008). Astronomers unveil wish list. Nature *456*, 427–428. https://doi.org/10.1038/456427a.

Silva, S.R.P. (2003). Properties of Amorphous Carbon (INSPEC).

Silva, S.R.P., Amaratunga, G.A.J., Woodburn, C.N., Welland, M.E., and Haq, S. (1994). Quantum size effects in amorphous diamond-like carbon superlattices. J. Appl. Phys. *33*, 6458–6465. https://doi.org/10.1143/JJAP.33.6458.

Silva, S.R.P., Carey, J.D., Khan, R.U.A., Gerstner, E.G., and Anguita, J.V. (2002). Chapter 9 – amorphous carbon thin films. In Handbook of Thin Films, *4*, H.S. Nalwa, ed (Elsevier), p403–506.

Srinivasan, D.K., Perry, M.E., Fielhauer, K.B., Smith, D.E., and Zuber, M.T. (2007). The radio frequency subsystem and radio science on the messenger mission. Space Sci. Rev. *131*, 557–571. https://doi.org/10.1007/s11214-007-9270-7.

Timoshenko, S.P., and Gere, J.M. (1989). Chapter 1. Beam-columns. In Theory of Elastic Stability, S.P. Timoshenko and J.M. Gere, eds. (Dover Publications), pp. 1–45.

Tryggvason, B.V., Duval, W.M.B., Smith, R.W., Rezkallah, K.S., Varma, S., Redden, R.F., and Herring, R.A. (2001). The vibration environment on the international space station: its significance to fluid-based experiments. Acta Astronaut *48*, 59–70. https://doi.org/10.1016/S0094-5765(00)00140-5.

Tsu, R. (2010). Superlattice to Nanoelectronics (Elsevier Oxford). https://doi.org/10.1080/00107514.2012.661774.

Utsunomiya, S., Kamiya, T., and Shimizu, R. (2013). Development of CFRP mirrors for space telescopes. In Proceedings of Material Technologies and Applications to Optics, Structures, Components, and Sub-systems 88370P International Society for Optics and Photonics. https://doi.org/10.1117/12.2023425.

Wypych, G. (2018). Handbook of Adhesion Promoters (Chemtec Publishing).

Zhang, X., Dabral, S., Chiang, C., McDonal, J.F., and Wang, B. (1995). Crystallinity properties of parylene-n affecting its use as an ILD in submicron integrated circuit technology. Adv. Mater. Microelectron. *270*, 508–511. https://doi.org/10.1016/0040-6090(95)06842-2.

Zhang, Y., Kim, Y., Gilbert, M.J., and Mason, N. (2018). Electronic transport in a two-dimensional superlattice engineered via self-assembled nanostructures. Nat. npj 2D Mater. Appl. *2*, 31. https://doi.org/10.1038/s41699-018-0076-0.

STAR★METHODS

KEY RESOURCES TABLE

REAGENT or RESOURCE	SOURCE	IDENTIFIER
Chemicals, peptides, and recombinant proteins		
Dimer di-para-xylylene [2.2] Paracyclophane (97 %),Synonom: Tricyclo [8.2.2.24,7] hexadeca-4,6,10,12,13,15-hexaene	Speciality Coating Systems A KISCO Company)	Cat# 1633-22-3
Acetylene	BOC	Cat# 74-86-2
Hydrogen	BOC	Cat# 1333-74-0

RESOURCE AVAILABILITY

Lead contact

Further information and requests for resources and reagents should be directed to and will be fulfilled by the lead contact, S. Ravi P. Silva (s.silva@surrey.ac.uk).

Materials availability

This study did not generate new unique reagents.

Data and code availability

This study did not generate/analyse data sets/code. All data are described in the main text and methods.

METHOD DETAILS

Deposition

Single PECLP and PECLP:DLC multilayers were deposited under vacuum using a custom-built PECVD coating system in which the substrate materials acted as a virtual electrode connected to the RF power supply. A poly (p-xylylene) dimer di-para-xylylene was used ([2.2] Paracyclophane) and pyrolyzed at 650°C to form the poly(p-xylylene) monomer and then introduced into the plasma within the PECVD chamber to form the PECLP. After PECPL deposition, the dimer source was closed off and a hydrogen acetylene mixture was introduced into the system, in which hydrogen acted as a carrier gas, carrying the acetylene precursor required for DLC deposition. For PECLP:DLC multilayer structure the initial layer was PECLP with the hard DLC layer deposited on it. The first PECLP buffer layer was typically 500 nm thick and the first DLC layer was 50, 100 or 200 nm thick. The second and subsequent coating layer(s) that were deposited on top of the initial PECLP:DLC layers combination were PECLP and DLC with the PECLP layer reduced from 500 to 100 nm. All layers were deposited continuously, without interrupting the plasma. The composition of the PECLP layer was confirmed using FTIR, which is shown in Figure S1.

Thermal-vacuum outgassing tests for screening of space materials

μ-VCM measurements were performed in a high vacuum at 65°C and 125°C. The measurements were performed according to the Space Product Assurance document (no.ECSS-Q-St-70-02C, European Cooperation for Space Standardization of space activities, https://ecss.nl/standard/ecss-q-st-70-02c-thermal-vacuum-outgassing-test-for-the-screening-of-space-materials/) in a dedicated and certified ESA laboratory in Madrid. The total amount of CVCM, such as water or volatile organic compounds (VOCs), was collected using a micro-balance plate cooled to 77K using LN_2 for analysis using infrared spectroscopy. This μ-VCM test was used to determine the outgassing screening properties of materials proposed for use in the fabrication of spacecraft and associated equipment. The outgassing was defined as the mass loss of a sample due to vacuum conditioning at elevated temperatures. Furthermore, the mass gain of cooled collectors due to condensed matter was measured. The infrared spectroscopy analyzed was done to evaluate the possible contamination of sensitive components by outgassed materials. The measurements were performed in the following steps:

- Pre-conditioning of samples: 24 hours at 22°C and 55%rH
- Weighing of samples (micro balance), empty sample cups and collectors
- Thermal vacuum test: 24 hours in vacuum ($P<10^{-5}$ mbar)
- Weighing of samples
- Final measurements and infrared inspection

The μ-VCM apparatus consisted of an insert located in vacuum system suitably dimensioned with respect to the insert, able to accommodate all the feedthroughs. The bake-out of the system was carried-out at min. temperature of 25°C above the maximum test temperature before the measurements to ensure cleanliness of the system. Each test covered minimum 3 composite plates per cup to fulfill the ECSS-Q-St-70-02C requirements.

Thermal-vacuum cycling tests

Thermal-vacuum cycling tests were performed several times during development exposing specimens up to 100 temperature cycles ranging from 77K to 523K with pre-defined holding times and temperature ramps. Additional thermal cycling from -50°C to 80°C was performed in a thermal-vacuum chamber (TS-70/600.10/s) used for space hardware with a heating rate of 10°C. This was realized in Germany space test facilities. Thermal couples were used during all tests to monitor the temperature, while the environment was achieved thanks to thermal shrouds and liquids which passed through them.

Adhesion verification w/wo thermal-shock test

The adhesion tape test has been applied after all coating runs as well as after the end of particular mechanical and environmental test campaigns to verify coating robustness and adhesion. This has been realized always on witness samples at the beginning of each test, and on tested samples at the end of the tests. At least 5 [cm] of pressure sensitive tape was attached on the surface of the test samples. The pressure has been applied to ensure it adhered well to the surface. The tape was then pulled at right-angles at a rate of approx. $1 cms^{-1}$. A reminisce of coating was then inspected on the tape. Additionally, all coated components were tested and required to pass adhesion tape test after undergoing thermal cycling in LN_2 (~ -200°C). At least 10 cycles from RT to LN_2 were applied.

Nano-identation characterization

Hardness and elastic modulus measurements on single PECLP and DLC layers were performed in ambient and atmospheric conditions using a nanoindentation system (Nanotest Xtreme, Micro Materials, UK). Indents were made with a sharp diamond Berkovich indenter (MicroStar, USA). Prior to testing, the instrument was calibrated (load, displacement and frame compliance) and the area function of the indenter was indirectly verified by conducting idents at different depth in a reference material (fused silica), in agreement with ISO 14577-1. All indents were performed in load-control, with a defined indentation profile. The maximum load was adjusted in order to reach a maximum depth of about 50-60nm to maintain the indentation stress field within the coating, avoiding substrate effect. The Oliver-Pharr method was used to extract hardness and elastic modulus values from each indent.

Contact pressure measurement on PECLP:DLC superlattice coatings were performed in ambient and atmospheric conditions using a nanoindentation system (Nanotest Xtreme, Micro Materials, UK). Indents were made with a sharp diamond Berkovich indenter (MicroStar, USA). The instruments were calibrated before testing (load, displacement and frame compliance) and the area function of the indenter was indirectly verified by conducting indents at different depth in a reference material (fused silica) in agreement with ISO 14577-1. All indents were performed in load-control, using a multi-loading cycle procedure consisting of 10 maximum loads (P1 to P10). The last maximum load, P10, was adjusted to reach a maximum depth of about 150 nm to maintain the indentation stress field within the coating and avoid substrate effect. The Oliver-Pharr method was used to extract hardness and elastic modulus values from each indent.

The in-situ nanoindentation tests were performed with the ASMEC UNAT-SEM II system inside a Carl Zeiss Auriga 60 FIB-SEM (Figure S2). The samples were mounted vertically, and the stage was tilted to 12° to view the surface with the electron beam. A cube corner conductive boron-doped diamond indenter tip was used for the nanoindentation. All the samples could be tested in the same session, removing any variation in the

results caused by setting up the apparatus more than once. The load-controlled profile was as follows: loading for 40 s up to 200 mN with a quadratic gradient, hold at maximum load for 30 s, unload to 10 mN with a linear gradient and hold for 60 s, unload to zero. The imaging conditions used for the electron beam were 5 kV accelerating voltage, 30 μm aperture and 19.5 mm working distance.

Thickness inspection measurements

A Dektak profilometer, optical microscopy and in-situ quartz oscillator methods were used to inspect and measure the coating thickness. The in-situ method is based on quartz oscillator microbalance (QMB) that displays thicknesses in the range from 0.1 [nm] – 100 [μm] and deposition rates from 0.01 – 100 nms-1. The mass determination is related to the change of the resonance frequency of an oscillating quartz crystal. After all coating runs a Dektakt profilometer from Bruker was used to verify (ex-situ) the precise thickness of thin films across the surfaces, down to the nanometer scale. The data were obtained from the industrial software provided by the apparatus.

Dilatometry measurements

A special high precision Netsch dilatometer constructed to measure composites and polymers materials was used to measure volume changes caused by physical or chemical processes. This allowed to study lengths change phenomena of materials and provided information about their thermal behavior. 30 unidirectional CFRP samples were used with plies oriented in 0° and 90° directions. The studied temperature was between -40°C and 80°C to maintain the typical operation temperature for space structures.

Three-point bending tests

The three-point bending tests were used to measure flexural properties of the coated and uncoated UHM CFRP materials and verify coating robustness. The tests were carried out in a mechanical Zwick machine 1474 in accordance to DIN EN ISO 14125 (Figure 4A), as follows:

- Load cell 10 kN
- Jig distance for UD0° CFRP: 80 mm
- Jig distance for 90° CFRP: 40 mm
- Cross head velocity for UD0°: 2 mm/min
- Cross head velocity for UD90°: 0.5 mm/min

In total 42 unidirectional composites were tested.

Vibration tests

Vibration tests were carried out in a small vibration shaker system V780 which allows excitation for space qualification tests on components and small assemblies level under controlled conditions. The elastic modulus calculated from these tests are summarized in Table S1. The system operates in the frequency range of DC to 4000 Hz from either sine or random vibration. Two input sensors have been allocated on the upper and lower parts of the mounting bracket. Accelerometers were used to measure generated peaks on the bracket and attached masses at the free-end of the beam (Table S2). The resonance search was performed to the following spectrum: frequency 10-2000 Hz, amplitude 0.2 g, sweep rate 2 Oct/min and sine vibration mode. In total 83 runs were carried out.